ELSEVIER

Biochimica et Biophysica Acta 1554 (2002) 5–21

BIOCHIMICA ET BIOPHYSICA ACTA
BBA

www.bba-direct.com

Review

Structure–function relationships in *Anabaena* ferredoxin/ferredoxin:NADP$^+$ reductase electron transfer: insights from site-directed mutagenesis, transient absorption spectroscopy and X-ray crystallography

John K. Hurley [a], Renaud Morales [b], Marta Martínez-Júlvez [c], Tammy B. Brodie [a], Milagros Medina [c], Carlos Gómez-Moreno [c], Gordon Tollin [a,*]

[a] *Department of Biochemistry and Molecular Biophysics, University of Arizona, 1041 E. Lowell Street, Tucson, AZ 85721-0088, USA*
[b] *Laboratoire de Cristallographie et de Cristallogénèse des Protéines, Institut de Biologie Structurale J.P. Ebel, CEA-CNRS, 41 rue Jules Horowitz, F38027 Grenoble, France*
[c] *Departmento de Bioquímica y Biología Molecular y Celular, Universidad de Zaragoza, 50009 Zaragoza, Spain*

Received 20 June 2001; received in revised form 25 January 2002; accepted 29 January 2002

Abstract

The interaction between reduced *Anabaena* ferredoxin and oxidized ferredoxin:NADP$^+$ reductase (FNR), which occurs during photosynthetic electron transfer (ET), has been investigated extensively in the authors' laboratories using transient and steady-state kinetic measurements and X-ray crystallography. The effect of a large number of site-specific mutations in both proteins has been assessed. Many of the mutations had little or no effect on ET kinetics. However, non-conservative mutations at three highly conserved surface sites in ferredoxin (F65, E94 and S47) caused ET rate constants to decrease by four orders of magnitude, and non-conservative mutations at three highly conserved surface sites in FNR (L76, K75 and E301) caused ET rate constants to decrease by factors of 25–150. These residues were deemed to be critical for ET. Similar mutations at several other conserved sites in the two proteins (D67 in Fd; E139, L78, K72, and R16 in FNR) caused smaller but still appreciable effects on ET rate constants. A strong correlation exists between these results and the X-ray crystal structure of an *Anabaena* ferredoxin/FNR complex. Thus, mutations at sites that are within the protein–protein interface or are directly involved in interprotein contacts generally show the largest kinetic effects. The implications of these results for the ET mechanism are discussed.

Keywords: Protein–protein interaction; Kinetic; Photosynthetic electron transfer; Transient complex; X-ray crystal structure

1. Introduction

Electron transfer (ET) reactions are ubiquitous in biological systems, and life as we know it would not exist without them. A non-heme iron protein ferredoxin and one of its ET partners, the flavoenzyme ferredoxin:NADP$^+$ reductase (FNR), function in photosynthetic ET. Ferredoxin is the terminal electron acceptor from Photosystem I and reduces FNR in two one-electron transfer steps. FNR uses these electrons to catalyze the two-electron reduction of NADP$^+$ to NADPH. This represents one of the main energy conversion processes in biology. The overall reaction is shown in Eq. (1).

$$2Fd_{red} + NADP^+ + H^+ \xrightarrow{FNR} 2\ Fd_{ox} + NADPH \quad (1)$$

The "plant-type" ferredoxins contain a [2Fe–2S] cluster as their prosthetic group in a polypeptide chain having 93–98 amino acids [1], giving them a molecular mass of about 11 kDa. The ferredoxin utilized in the present studies has been isolated from vegetative cells of *Anabaena* PCC 7120 and has a molecular mass of 10.7 kDa. FNR as isolated

Abbreviations: DCPIP, 2,6-dichlorophenolindophenol; dRf, 5-deazariboflavin; dRfH•, 5-deazariboflavin semiquinone radical; ET, electron transfer; Fd, wild-type *Anabaena* 7120 vegetative ferredoxin; Fd_{ox}, oxidized ferredoxin; Fd_{red}, reduced ferredoxin; Fd_{sp}, spinach ferredoxin; FNR, ferredoxin:NADP$^+$ reductase; FNR_{ox}, oxidized FNR; FNR_{red}, reduced FNR; FNR_{sp}, spinach FNR; FNR_{sq}, FNR semiquinone; INT, 2-(*p*-iodophenyl)-3-nitrophenyl-5-phenyltetrazolium chloride; k_{obs}, observed first-order rate constant; natFNR, native *Anabaena* 7119 FNR; P-AMP, adenosine-2′, 5′-diphosphate; recFNR, wild-type recombinant *Anabaena* 7119 FNR; VDW, van der Waals; μ, ionic strength; wt, wild-type

* Corresponding author. Tel.: +1-520-621-3447; fax: +1-520-621-9288.
E-mail address: gtollin@u.arizona.edu (G. Tollin).

0005-2728/02/$ - see front matter
PII: S0005-2728(02)00188-3

from the closely related *Anabaena* PCC 7119 is a 36-kDa protein containing one FAD molecule as cofactor. This is a truncated version of the complete 49 kDa petH gene product [2,3], which is proteolytically cleaved during isolation.

High-resolution structures have been determined for several plant-type ferredoxins (Table 1), including an isoform of ferredoxin present in heterocyst cells of cyanobacteria that is involved in N_2-fixation [17]. The *Anabaena* 7120 heterocyst ferredoxin is 51% identical to the vegetative form that functions in photosynthetic ET. X-ray crystal structures are also available for FNRs from various other sources (Table 2).

Several plausible computer models of ferredoxin/FNR complexes have been generated on the basis of these X-ray structures and biochemical information, e.g. [23,25,26]. In addition, crystal structures of complexes formed between $NADP^+$ and pea FNRs mutated at the C-terminal residue (Y308) have been reported [22], providing the first three-dimensional view of the interaction between FNR and its non-protein substrate. Recently, a 2.4-Å resolution X-ray structure of a ferredoxin/FNR complex between the oxidized forms of wild type (wt) *Anabaena* ferredoxin and wt *Anabaena* 7119 FNR has been reported [27], as has a 2.9-Å resolution structure of a complex between oxidized ferredoxin and FNR from maize [21].

Table 1
[2Fe–2S] ferredoxin structures[a]

Source	Resolution (PDB code)
Aphanothece sacrum[b]	2.2 Å (1FXI)
Anabaena 7120 (vegetative)[c]	2.5 Å (1FXA)
Anabaena 7120 (heterocyst)[d]	1.7 Å (1FRD)
Equisetum arvense[e]	1.8 Å (1FRR)
Spirulina platensis[f]	2.5 Å (4FXC)
Haloarcula marismortui[g]	1.9 Å (1DOI)
Spinacia oleracea (mutant E92K)[h]	1.7 Å (1A70)
Chlorella fusca[i]	1.4 Å (1AWD)
Anabaena 7119 (vegetative)[j]	1.3 Å (1QT9)
*Anabaen*a 7119 (vegetative–reduced)[j]	1.2 Å (1CZP)
Synechocystis sp. PCC 6803[k]	(1DOX)
Synechococcus elongatus[l]	(1ROE/2CJO)
Parsley[m]	(1PFD)

[a] These structures were determined by X-ray diffraction, except for the *Synechocystis*, *Synechococcus* and parsley structures, which were determined by NMR. All structures are for the oxidized forms of the proteins, except where otherwise noted.
[b] From Ref. [4].
[c] From Ref. [5].
[d] From Ref. [6].
[e] From Ref. [7].
[f] From Ref. [8].
[g] From Ref. [9].
[h] From Ref. [10].
[i] From Ref. [11].
[j] From Ref. [12].
[k] From Ref. [13].
[l] From Refs. [14,15].
[m] From Ref. [16].

Table 2
Ferredoxin:$NADP^+$ reductase structures[a]

Source	Resolution (Å) (PDB Code)
Anabaena 7119[b]	1.8 (1QUE)
A. vinelandii[c]	2.0 (1A8P)
E. coli[d]	2.2 (1QFJ)
Maize[e]	2.2 (1GAW)
Pea[f]	2.5 (1QG0)
Pea/$NADP^+$[f,g]	1.8 (1QFY)
Paprika[h]	2.5 (1FB3)
Spinach[i] (reduced)	1.7 (1FNC)
Spinach[i]	1.7 (1FNB)
Spinach/P-AMP[i,j]	1.7 (1FND)

[a] These structures were determined by X-ray diffraction. All proteins were in their oxidized forms, except for where indicated.
[b] From Ref. [18].
[c] From Ref. [19].
[d] From Ref. [20].
[e] From Ref. [21].
[f] From Ref. [22].
[g] This structure is for the Y308S mutant complexed with $NADP^+$. The structure of Y308S in complex with NADPH has also been solved (PDB code 1QFZ), as has the Y308W mutant in complex with $NADP^+$ (PDB code 1QGA).
[h] From Ref. [23].
[i] From Ref. [24].
[j] This structure is for the protein complexed with 2′-phospho-5′-AMP.

Early studies [28] described the formation of complexes between various ferredoxins and spinach FNR (FNR_{sp}) and pointed to the importance of electrostatic interactions in the functioning of these proteins. Subsequent investigations [29] confirmed these findings and postulated the existence of regions of positive charge on FNR_{sp} interacting with negative charges on ferredoxin. In agreement with this, studies of ionic strength (μ) effects on the kinetics of ET from spinach ferredoxin to FNR_{sp} using laser flash photolysis [30,31] indicated a strong influence of complementary electrostatic charges on complex formation and stabilization and ET rate constants. Many subsequent results from our laboratories (see below) are consistent with a plus–minus electrostatic interaction between the proteins from *Anabaena*. Additionally, thermodynamic studies have shown that hydrophobic effects also contribute to complex stability in the spinach proteins [32], and differences between experimental and theoretical complex stability constant values as a function of μ have been attributed to hydrophobic interactions in the *Anabaena* proteins [33]. In agreement with these results, the crystal structure of the complex formed between the *Anabaena* proteins revealed that the molecular interface includes a hydrophobic core involving the side chains of F65 from Fd and L76, L78 and V136 from FNR [27,34]. As will be described below, the combined role of electrostatic and hydrophobic interactions is strongly supported by kinetic studies involving site-specific mutations of the *Anabaena* proteins.

Early transient kinetic results on the ET reaction from Fd to *Anabaena* FNR [31,35] are consistent with a (minimal) two-step mechanism consisting of complex formation

followed by ET. This is shown in Eq. (2), where K_d and k_{et} represent the dissociation constant for the transient complex and the ET rate constant, respectively. It should be emphasized that k_{et} includes factors such as possible protein structural rearrangements and changes in hydration of the proteins occurring upon redox state changes and complex formation, as well as the intrinsic ET rate constant.

$$Fd_{red} + FNR_{ox} \overset{K_d}{\rightleftharpoons} [Fd_{red} - FNR_{ox}] \overset{k_{et}}{\rightarrow} Fd_{ox} + FNR_{red} \quad (2)$$

Inasmuch as the X-ray crystal structures of *Anabaena* 7120 ferredoxin [5] and *Anabaena* 7119 FNR [18] are available, and the proteins from these organisms have been cloned and overexpressed in *Escherichia coli* [36–40], they are excellent candidates for studies of structure–function relationships in ET proteins. It is not the intention of this paper to comprehensively review the literature on these proteins (reviews are available on ferredoxin [41–43 and references therein] and on Fe–S proteins in general [44–46 and references therein], as well as on FNR [47–50 and references therein]). Rather, we will focus on the research that has taken place in the authors' laboratories over the past 10 years, utilizing site-directed mutagenesis, transient absorbance spectroscopy and X-ray crystallography. Results obtained with some of the mutants described here have appeared in earlier reviews [51–53]. In addition, some results are presented here for the first time (Fd mutants D28, E31, E32, D36, F39, S40, H92 and Y98). Although a large body of literature exists on mechanisms of protein–protein ET [54–61], it is beyond the scope of this paper to review this literature.

Fig. 1 shows space-filling representations of the "front" surfaces (i.e. the surfaces to which the prosthetic groups are closest) of Fd (panels A, B) and FNR (panels C, D), respectively. In Fig. 1A and C, those residues that have been mutated in the present studies are color-coded, with red being used for those showing large kinetic effects on ET between FNR and Fd upon non-conservative mutation, green for those showing moderate kinetic effects, and blue for those showing minimal effects on ET reactivity (see legend to Fig. 1 for details; this color-coding is based on the relative reactivities given below in Tables 5 and 6). Although this classification is somewhat arbitrary, it allows us to compare kinetic results with structural findings.

In Fig. 1B and D, residues found to be at the protein–protein interface in the crystalline complex [27] are colored red. As will be discussed below, good correspondence is found between the effects that the mutations had on ET reactivity and their presence at the complex interface. A representation of the crystalline complex is shown in Fig. 2A, and a more detailed view of the interfacial region is shown in Fig. 2B. This will be discussed further below.

2. Goals and strategies

The general goal of the research described herein was to identify those residues in Fd and *Anabaena* FNR that were involved in the mutual interaction of these proteins leading to complex formation and ET. It should be noted that the crystal structure of the complex was not solved until relatively recently [27], and thus most of the kinetic work was done prior to this. Site-directed mutagenesis was applied to highly conserved [62–67] charged and hydrophobic surface residues that are in the vicinity of the redox cofactors. In most cases, both non-conservative (e.g. charge-reversal) and conservative mutations were made. Residues were also chosen for mutation based on cross-linking and chemical modification studies of Fd_{sp} that suggested the involvement of *Anabaena* residues in the regions 28–32, 67–72 and 94–96 [26,68,69]. Additionally, computer modeling [25,26] based on the crystal structures of FNR_{sp} and *Spirulina* Fd also points to acidic residues in these segments of the Fd molecule. Biochemical studies on spinach [68,70] and *Anabaena* FNRs [71,72] have implicated *Anabaena* residues K72 and K138 in binding Fd. Several residues [73] in the [2Fe–2S] cluster binding loop of Fd (residues 39–50) were also targeted for mutation.

The effects of a given mutation were studied by a number of techniques. Laser flash photolysis/time-resolved absorbance was used to measure the rate constants for reduction of the oxidized mutant proteins by 5-deazariboflavin semiquinone radical (dRfH•, Section 3), and to directly measure the binding constant and the ET rate constant for the interaction between Fd_{red} and FNR_{ox} for a mutant and its non-mutated partner. These latter experiments were done as a function of μ at constant protein concentration, or as a function of FNR concentration at constant μ and Fd concentration. ET reactivities (k_{obs} values) measured in this way, relative to the reactivity of the non-mutated protein, were used to judge whether a particular mutation altered the redox behavior of the cofactor or was crucial to the protein–protein ET interaction. Stopped-flow and steady-state kinetic measurements were also made in some cases.

UV–VIS absorption and CD spectra of the mutant proteins were routinely measured. Except for the mutations of the Cys residues that ligate the [2Fe–2S] cluster in Fd (Section 4.2), such spectra for all mutants were essentially identical to the corresponding non-mutated protein, indicating that the cofactor environments were not appreciably altered.

Reduction potentials of Fd and FNR, alone and in a 1:1 complex, have been measured by potentiometric titration, as have the potentials for several Fd [73,74] and FNR mutants [64]. The values are given in Tables 3 and 4. For several other FNR mutants the reduction potentials for the oxidized/semiquinone couple ($E_1{}^{\circ\prime}$) were estimated by comparing the concentrations of FNR required to fully reoxidize Fd_{red}. For all mutants in which ET reactivity was decreased, altered reduction potentials were ruled out as the cause. It should be

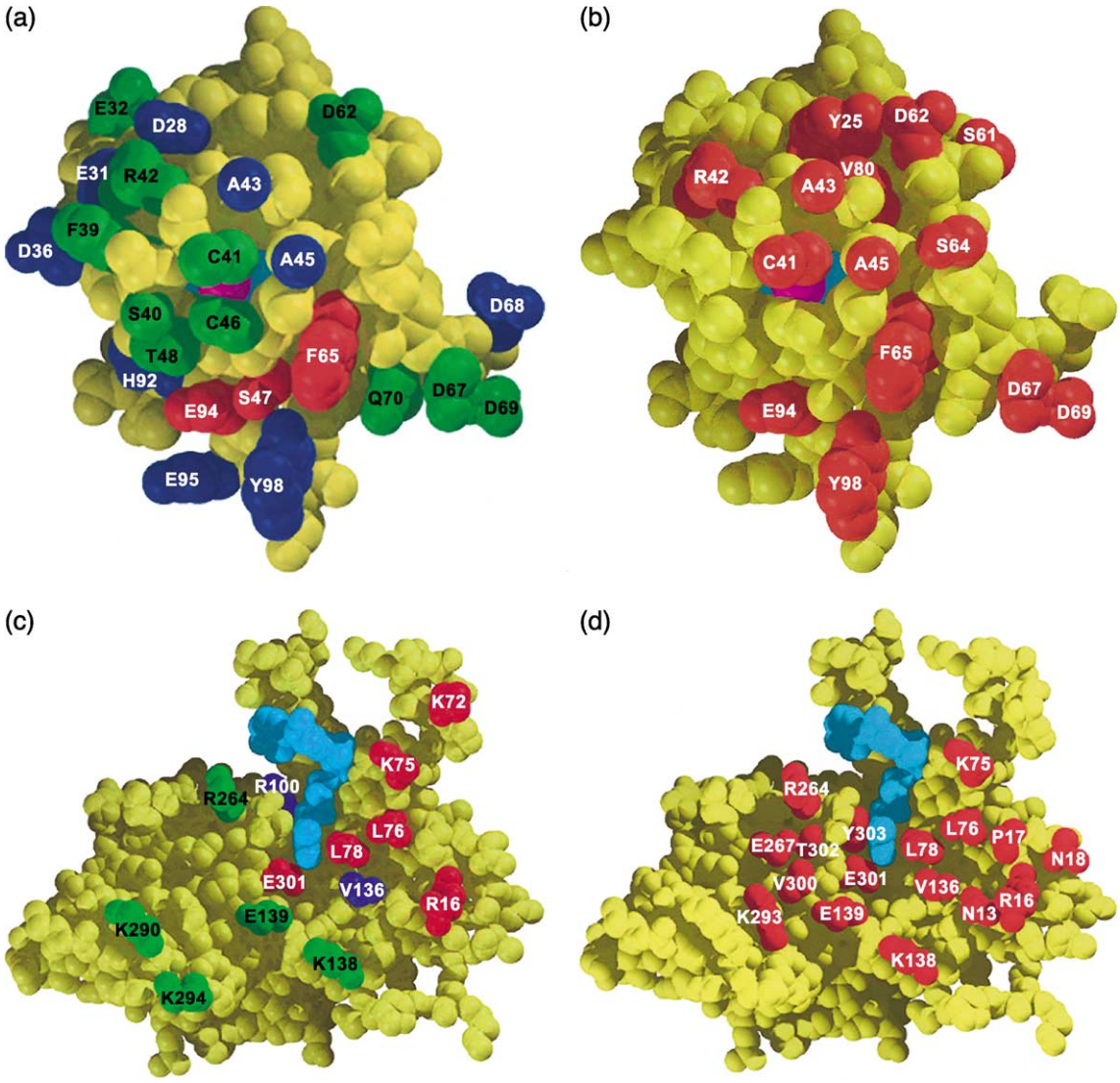

Fig. 1. Space-filling representation of the front surfaces of *Anabaena* Fd (a, b) and *Anabaena* FNR (c, d). The [2Fe–2S] cluster of Fd can be seen at approximately the middle of the Fd molecule. Fe1 of the cluster is shown in magenta and S1 and S2 are shown in blue to the left and right of Fe1, respectively. The FAD cofactor of FNR is shown in blue. In (a) and (c), residues showing large kinetic effects (cf. Tables 5 and 6) upon mutation are shown in red, those showing moderate effects are shown in green and those showing small or no effect are shown in blue. In this scheme, reactivities which were $> \sim 70\%$, $\sim 15\%$ to $\sim 70\%$ and $< \sim 15\%$ as effective as the non-mutated Fd/FNR system were considered to have small, moderate and large kinetic effects, respectively. If multiple mutations were made at a given residue, then evaluation of the importance of the residue for ET was based on the reactivity of the least reactive mutation at that site. C49 of Fd is colored green in (a) but cannot be seen in this view because it is on the other side of the [2Fe–2S] cluster. In (b) and (d) the side chains of residues present at the Fd/FNR complex interface are shown in red. C46, S47 and T48 of Fd are not colored red in (b). Although C46 and S47are positioned in front of FNR, a cavity is present between the two proteins in this region, and T48 interacts with FNR but the distances are quite large (>5.8 Å). In FNR (d), G137 is at the interface but is not colored due to the nature its side chain. Coordinates were obtained from the Protein Data Bank (1FXA for Fd [5] and 1QUE for FNR [18]).

noted that complex formation between Fd and FNR caused shifts in the reduction potentials (Table 3). In some cases, such shifts caused otherwise thermodynamically unfavorable ET reactions to become either isopotential (e.g. E94K) or favorable (e.g. S47A). In other cases (e.g. F65A and E49Q), it was presumed that complex formation would render the reactions thermodynamically favorable. Additionally, in the kinetic experiments the ratio of FNR_{ox} to Fd_{red} was greater than 30:1, which would compensate for at least 90 mV of unfavorable potential difference. For FNR mutants whose reduction potentials were not directly measured but which showed decreased ET activity (K75E, L78A, K138E, E301A), the estimated one-electron reduction potentials were either similar to that of wt FNR or the estimated unfavorable potential shift was not sufficient to account for the decrease in the observed ET rate constant.

X-ray crystal structures were determined for several Fd mutants (S47A, D62K, D68K, E94K, E95K, Q70K [74], and C49S [75]). In no cases were significant alterations in the structure relative to Fd observed. The RMS deviations of

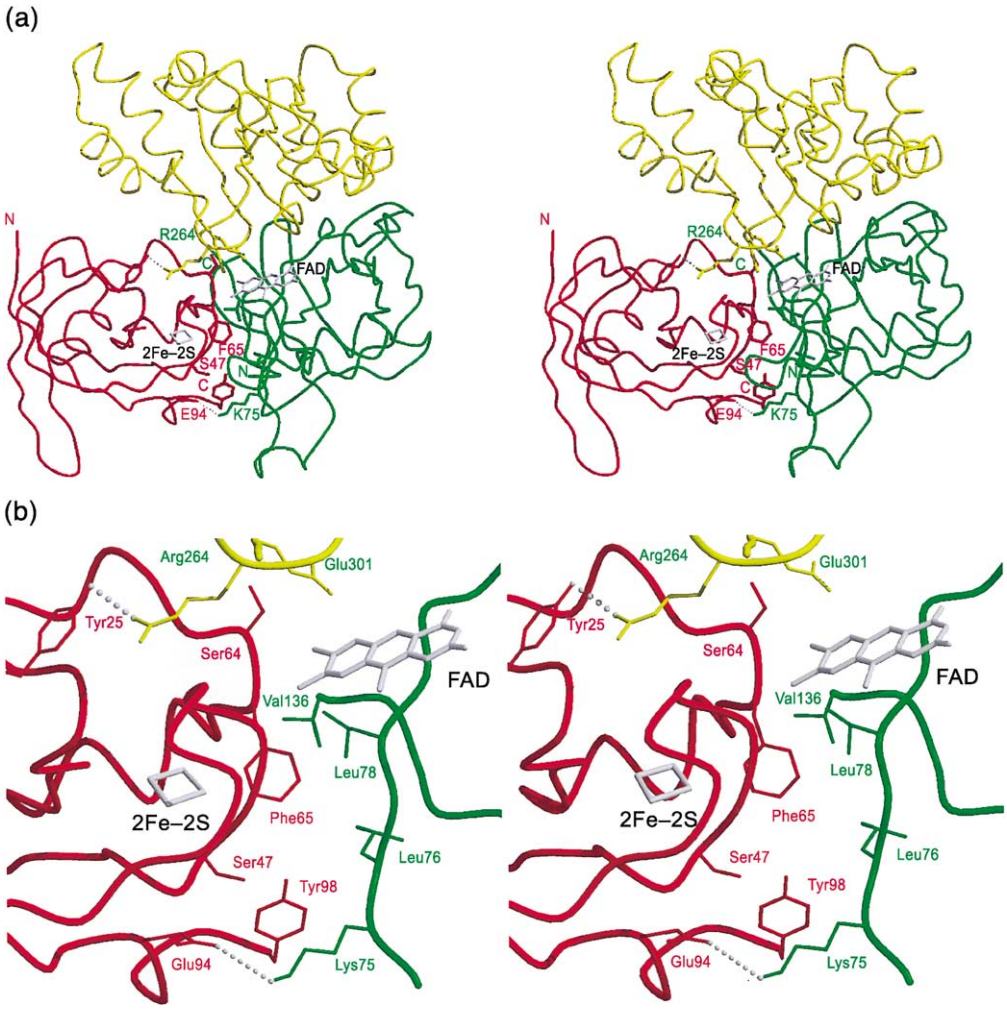

Fig. 2. (a) Stereo representation of the crystalline complex formed between the *Anabaena* FNR and Fd including the respective FAD and 2Fe–2S cofactors (in gray), main chain traces and side chains which play the most crucial role in the interaction (see text). Two typical intermolecular hydrogen bonds are also drawn in dotted lines. Fd is colored in red, the N-terminal FNR FAD binding domain in green and the C-terminal $NADP^+$ binding domain in yellow. This figure was created using MOLSCRIPT2 [107] and RASTER3D [108]. The coordinates are available from the Protein Data Bank (1EWY). (b) Close-up stereo view of the interface region of the Fd/FNR complex in the vicinity of the redox cofactors.

the C^{α} backbones of the mutant structures relative to Fd were in the range 0.12–0.41 Å, with the larger values being ascribed to differences in crystal packing. Structures were also determined for several FNR mutants (E301A [76], R264E [66], L78D, L76D/L78D and V136L [64]). All of these structures were essentially identical to wt *Anabaena* FNR except that in the structure of E301A, another residue (E139) adopted a slightly different conformation (see Section 5.1 for discussion). Based on these results, as well as on the UV–VIS and CD spectra, in all cases where reactivity was decreased, structural changes in the mutant protein were ruled out as the cause.

3. Reaction of Fd with native and recombinant FNR

Early experiments were carried out with native FNR (natFNR) and more recent experiments utilized recombinant FNR (recFNR). It should be noted that these two species react differently [33,77] at low μ (Fig. 3). This was attributed to the presence at the N-terminus in recFNR of six amino acids (TQAKAK) that are proteolytically cleaved during isolation of the native protein. The presence of two additional positive charges apparently causes the highly negatively charged Fd to form an intermediate complex with recFNR at low values of μ that is less optimal for ET than the intermediate complex involving natFNR, although in both cases, the complex formed at low μ is less reactive than at higher μ values. As μ is increased, the complex is weakened, allowing the proteins to assume more optimal mutual orientations for ET. After the maximal observed ET rate constant (k_{obs}) is reached, further increases in μ result in decreases in k_{obs} as expected due to screening of the oppositely charged residues on the protein surfaces, which diminishes long-range electrostatic attractive forces. Thus, the overall μ dependence is biphasic.

Table 3
Influence of complex formation on the reduction potentials of FNR and some Fd mutants[a]

Ferredoxin		FAD of FNR (mV)			[2Fe–2S] of Fd (mV)
		$E_1^{\circ\prime}$	$E_2^{\circ\prime}$	$E_m^{\circ\prime}$	$E^{\circ\prime}$
None		−331	−314	−323	–
Fd	alone	–	–	–	−384
	complexed	−291	−300	−298	−372
	ΔE	+40	+14	+25	+12
F65I	alone	–	–	–	−328
	complexed	−277	−273	−274	−338
	ΔE	+54	+41	+49	−10
E94K	alone	–	–	–	−304
	complexed	−291	−286	−282	−298
	ΔE	+40	+28	+41	+15
S47A	alone	–	–	–	−337
	complexed	−269	−282	−273	−336
	ΔE	+62	+32	+50	+1

[a] Taken from Ref. [74]. The pH was 7.5 and the temperature was 4 °C. For measurements on the complexed proteins, μ was approximately 12 mM. For measurements on the uncomplexed proteins, μ was approximately 100 mM. Typical uncertainty in the measurements is 1–3 mV.

Relative values of k_{obs} for mutant proteins were taken from plots of the μ dependency of k_{obs} (such as those shown in Fig. 3) and were normalized to the same FNR concentrations. The value of μ at which the k_{obs} value was taken corresponded to the μ value at which the reference FNR reached its maximum value (i.e. $\mu = 40$ mM for natFNR and $\mu = 110$ mM for recFNR; see Fig. 3). Note that the maximal k_{obs} values for both proteins are the same (4600 ± 400 s^{-1} for natFNR and 4500 ± 400 s^{-1} for recFNR).

Table 4
Reduction potentials of Fd and Fd mutants and midpoint two-electron reduction potentials of isolated recFNR and mutant FNRs[a]

Ferredoxin	$E^{\circ\prime}$ (mV)	Ferredoxin	$E^{\circ\prime}$ (mV)	FNR	$E_m^{\circ\prime}$ (mV)
Fd[b]	−384	F65I[b]	−328	recFNR[c]	−323
R42H[d]	−382	F65Y[b]	−390	L76D[c]	−330
A43S[d]	−381	D68K[b]	−380	L76F[c]	−333
A45S[d,e]	−375	Q70K[b]	−382	L76S[c]	−305
C46S[f]	−381	T78A[d]	−345	L76D/L78D[c]	−317
S47A[b]	−337	T78I[d]	−337	L78D[c]	−302
S47T[b]	−438	T78S[d]	−378	L78F[c]	−307
T48A[d]	−382	E94D[b]	−367	L78S[c]	−286
T48S[d]	−401	E94K[b]	−304	V136S[c]	−305
C49S[f]	−329	E94Q[b]	−319		
D62K[b]	−373	E95K[b]	−372		
F65A[b]	−291				

[a] Typical uncertainty in the measurements is 1–3 mV. Values relative to the standard hydrogen electrode (SHE).

[b] Taken from Ref. [74]. The pH was 7.5 and the temperature was 4 °C. The value of μ was approximately 100 mM (the potential measured for Fd at $\mu = 12$ mM was very similar to the 100 mM value).

[c] Taken from Ref. [64]. Measurements were made in 50 mM Tris–HCl buffer, pH 8 at 10 °C.

[d] Taken from Ref. [73]. Measurements were made in 50 mM potassium phosphate buffer, pH 7.5 at 4 °C.

[e] In agreement with Ref. [109].

[f] Taken from Ref. [75]. Conditions as in footnote b.

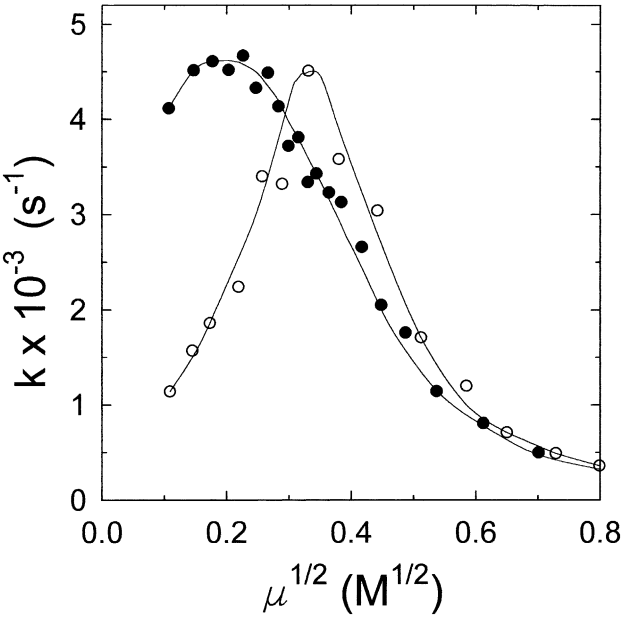

Fig. 3. The dependence of k_{obs} on μ for the ET reaction between Fd and natFNR (●) and recFNR (○). These data are adapted from Ref. [33]. The experiment using natFNR contained 30 μM Fd and 30 μM FNR. The experiment using recFNR contained 40 μM Fd and 30 μM FNR. Solutions also contained 0.1 mM 5-deazariboflavin and 1 mM EDTA in 4 mM potassium phosphate buffer, pH 7.0. μ was adjusted using aliquots of 5 M NaCl. Transient kinetics were monitored at 600 nm.

The means of generating Fd_{red} [78–80] involves the reaction of Fd_{ox} with the highly reducing, laser flash-generated dRfH•. All of the Fd and FNR mutants studied to date (the only exception is the E301A mutant of FNR, which apparently forms an intermediate complex with dRfH• [63]), react with dRfH• with rate constants that are very similar to the rate constants obtained for the unmutated proteins. Fd reacts with dRfH• with a second-order rate constant of $2.2 \pm 0.2 \times 10^8$ M^{-1} s^{-1}. The average value for the Fd mutants studied here is $1.6 \pm 0.3 \times 10^8$ M^{-1} s^{-1}. RecFNR and natFNR react with dRfH• with second-order rate constants of $2.1 \pm 0.2 \times 10^8$ M^{-1} s^{-1} and $2.2 \pm 0.2 \times 10^8$ M^{-1} s^{-1}, respectively. The average value for the FNR mutants studied here is $2.2 \pm 0.5 \times 10^8$ M^{-1} s^{-1}. These results are taken as an indication that the accessibility and intrinsic reactivity of the redox cofactors in the mutants have not been appreciably perturbed.

In protein–protein ET studies of systems following the mechanism described by Eq. (2), saturation is expected in a plot of k_{obs} vs. protein concentration, as the rate-limiting step switches from complex formation to ET at increased protein concentrations. In such cases, k_{et} and the value of K_d for the intermediate ET complex (Fd_{red}:FNR_{ox}) can be extracted from the kinetic data by fitting to the exact solution of the differential equation describing Eq. (2) [81,82]. Such saturation kinetics were observed at $\mu = 100$ mM for the reaction between Fd_{red} and both $natFNR_{ox}$ and $recFNR_{ox}$, and the values of k_{et} and K_d were found to be 5500 s^{-1} and 1.7 μM, respectively, for both proteins [33].

Thus, these two forms of FNR are kinetically indistinguishable at $\mu = 100$ mM.

4. Kinetic assessment of the importance of various amino acid residues in Fd

In the following discussion, critical, moderately important and unimportant residues are listed in sequential order within each group, except for the ligating Cys residues, which are presented together. This same general outline is followed for the FNR mutants in Section 5.

4.1. Critical Fd residues—S47, F65, E94

Non-conservative mutations at each of these positions caused a decrease of more than four orders of magnitude in the rate constant for ET with natFNR (Table 5). S47 is hydrogen-bonded to E94 in Fd and this hydrogen bond is part of a larger network of hydrogen bonds and electrostatic interactions that stabilizes the protein by anchoring the [2Fe–2S] binding loop to the protein [51]. In the crystalline complex, S47 does not interact directly with FNR although it lies within the Fd–FNR interface [27] (Fig. 2B).

The S47T mutant was constructed to assess the importance of the side chain hydroxyl group of this residue. Significantly, this mutation restored reactivity to about 50% of that determined for Fd (Table 5). Thus, it appears that a hydroxyl-containing side chain is required at position 47 in Fd for rapid ET with natFNR. Presumably, the hydrogen-bonding capability is retained by S47T. It would appear then that disruption of the hydrogen bond with E94 in the S47A mutation contributes significantly to the high degree of impairment observed for ET with this mutant.

Both the F65A and F65I mutants were essentially unreactive compared to Fd (Table 5). The dissociation constant for the complex of oxidized F65A with oxidized natFNR was approximately 10-fold larger than for Fd (120 vs. 9.4 μM) [35]. This K_d value is almost five times larger than that found for E94K (see below), which suggests the importance of hydrophobic interactions involving F65 in the complex with natFNR. However, a change in binding of this magnitude is not sufficient to account for the dramatic decrease in ET reactivity observed for F65A.

To further investigate the nature of the protein–protein interaction at this position, the mutants F65Y, F65W and S64Y/F65A were constructed [83]. F65Y was just as effective as Fd in ET with natFNR, whereas F65W was somewhat decreased in reactivity, although to a much smaller degree than F65I and F65A (Table 5). These results indicate that an aromatic side chain is required at position 65 for effective ET with natFNR. The S64Y/F65A double mutant was just as ineffective at transferring electrons to natFNR (Table 5) as were the F65A and F65I single mutants. Thus, an aromatic residue at the preceding position in the sequence could not substitute for F65, indicating a precise complementarity at

Table 5
Relative reactivities of Fd mutants in their ET reactions with FNR as studied by laser flash photolysis[a]

Fd	k_{obs}	Fd	k_{obs}	Fd	k_{obs}
D28K[b]	1.04	S47T[c]	0.50	D68K/D69K[d]	0.54
E31K[b]	0.87	T48A[e,f]	0.58	D69K[d]	0.57
E31K/E32K[b]	0.54	T48S[e,f]	1.00	Q70K[c]	0.59
D36K[b]	1.04	C49S[e,g]	0.47	T78A[e,f]	0.68
F39A[b]	0.67	D62K[c]	0.35	T78I[e,f]	0.75
S40A[b]	0.61	S64Y/F65A[h]	0.000065	T78S[e,f]	0.84
C41S[e,g]	0.39	F65A[h,i]	0.000065	H92E[b]	1.10
R42A[i]	1.54	F65I[h,i]	0.000087	E94D[j]	0.76
R42E[i]	0.54	F65W[b]	0.63	E94K[i]	0.000052
R42H[i]	1.17	F65Y[h]	1.00	E94Q[j]	0.000054
A43S[b]	0.83	D67K[d]	0.43	E95K[i]	1.03
A45S[b]	0.93	D67K/D68K/D69K[d]	0.20	E94K/E95K[b]	0.00013
C46S[e,g]	0.25	D67K/D69K[d]	0.20	Y98A[b]	0.91
S47A[c]	≤ 0.00005	D68K[d]	1.20		

[a] These observed first-order rate constants are relative to the natFNR/Fd ET reaction in cases where natFNR was used or to the recFNR/Fd ET reaction in cases where recFNR was used. The ionic strength at which the k_{obs} values were compared was 40 mM for cases where natFNR was used and 100 mM for cases where recFNR was used. These are the μ values at which the natFNR/Fd or recFNR/Fd reactions showed maximal reactivity. The FNR concentrations were normalized to the same concentration (30 μM; the vast majority of the experiments were performed at this concentration).

[b] These values have not been reported previously.

[c] From Ref. [74].

[d] From Ref. [90].

[e] No μ dependency was measured for these mutants and the k_{obs} values used were the 30 μM points from the FNR concentration dependency curves of k_{obs}.

[f] From Ref. [73].

[g] From Ref. [75].

[h] From Ref. [83].

[i] From Ref. [35].

[j] From Ref. [110].

the interface between the two proteins, as is seen in the crystalline complex [27]. We conclude that specific protein–protein interactions, which control the mutual orientations of the proteins within the intermediate ET complex and are altered by amino acid changes in the interfacial region are most likely the predominant factor leading to the kinetic impairment observed for these mutants. The proximity of the F65 side chain to the redox cofactors of Fd and FNR in the crystalline complex is shown in Fig. 4. Also shown in this figure are the L76 and L78 residues of FNR that interact with F65, as well as the charge-paired Fd E94–FNR K75 side chains (see below for further discussion).

In the X-ray crystal structure of parsley Fd [16] the phenyl ring of F63 (equivalent to F65 in *Anabaena* Fd) was found to be rotated 90° relative to that found in *Anabaena* Fd. The authors suggest "that while an aromatic ring in this position may be important, its orientation may not be." In addition, the Y63 residue of maize Fd (equivalent to F65 in *Anabaena*) has been shown in the crystal structure of the complex of the maize proteins [21] to be neither close to the [2Fe–2S] cluster of Fd nor situated between the prosthetic groups of the proteins. This will be discussed further below. Unfortunately, ET rate constants have not been determined for these proteins.

ET from $E94K_{red}$ to $natFNR_{ox}$ was highly impaired relative to Fd (Table 5, Fig. 5), as was also the case for E94K/E95K. Since E95K reacts like Fd (see Section 4.3, Table 5), the E94K mutation was responsible for the reduced reactivity of the double mutant. The E94 side chain is folded on the protein surface due to its formation of a hydrogen bond with Ser47 both in the isolated Fd structure and in the crystalline complex [5,27].

Another possible source of the change in reactivity is the protein–protein affinity during complex formation. The binding constant of $E94K_{ox}$ to $natFNR_{ox}$ [35] was found to be about a factor of three larger than the K_d value measured for Fd. Such a small change clearly cannot account for the four orders of magnitude decrease in ET reactivity observed for E94K. Due to the low reactivity of this mutant, it was not possible to determine K_d for the complex with Fd_{red}.

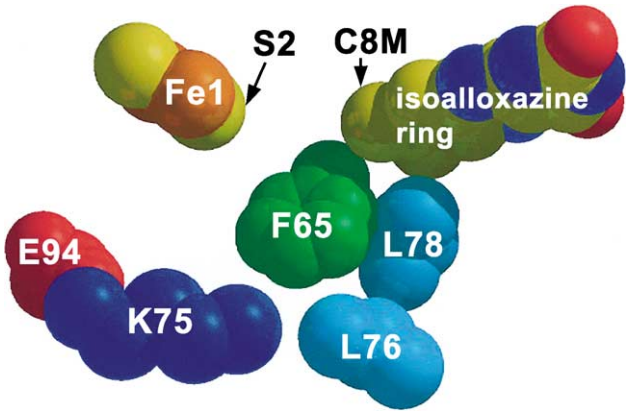

Fig. 4. Space-filling model showing the relative orientations of F65 of Fd and L76 and L78 of FNR with respect to the redox cofactors of the proteins. Also shown are the salt-bridged Fd E94 and FNR K75 residues. The distances from the C8-methyl (C8M) atom of the FAD to S2 (closest atom of the [2Fe–2] cluster) and to Phe65 Cα are 7.4 and 3.8 Å, respectively. Coordinates were obtained from the Protein Data Bank (1EWY [27]).

E94D reacted with natFNR much like Fd did (Table 5). E94Q, on the other hand, was just as impaired in its reaction with natFNR as was E94K (Table 5). These experiments clearly demonstrate the requirement of a negative charge at position 94 in Fd for rapid ET to natFNR.

As noted above, X-ray crystallography has shown that the E94 side chain in Fd is hydrogen-bonded to the side chain of S47 [51,74]. Thus, loss of this hydrogen bond due to the E94K mutation may contribute to the ineffectiveness of this mutant in ET with natFNR, as was the case with the S47A mutant. However, this is probably not a factor in the low reactivity of the E94Q mutant.

The equivalent residue to E94 in spinach Fd is E92. EPR spectroscopy, electrochemistry and steady-state kinetic studies have been carried out on the E92K, E92Q and E92A mutants [84–86]. The E92K mutation did not impair ET in a non-physiological assay in which ET occurs in the opposite direction. In contrast, in photoreduction of FNR by thylakoid membranes [85], E92Q and E92A were 58% and 53%, respectively, as effective as wt Fd_{sp}, whereas E92K was only 30% as effective. This was attributed to a less negative reduction potential for these Fd_{sp} mutants. It is important to point out that in such steady-state experiments, it is not known what the rate-determining step is, and thus it is possible that the observed rates do not reflect the Fd_{sp} to FNR ET step. Furthermore, it is not known to what extent redox potential shifts occur upon complex formation in these proteins. Based on the X-ray structure of E92K [10], it was determined by modeling a Glu residue at position 92 that the acidic side chain would be well-positioned to hydrogen bond with S45 (equivalent to S47 in *Anabaena*). Loss of this hydrogen bond in the E92K mutant protein may have a deleterious effect on the functionality of the spinach protein, similar to that observed for *Anabaena* Fd.

The above results demonstrate that for the *Anabaena* proteins, a negatively charged side chain is required at position 94 for effective ET with natFNR. In the crystal structure of the complex [27], E94 is clearly interacting with K75 of FNR at the FNR–Fd interface, presumably via a salt linkage. Consistent with this, as will be shown below, the K75E mutation in FNR resulted in a protein that was more than two orders of magnitude less effective in ET with Fd (see Section 5.1).

4.2. Moderately important Fd residues—E32, F39, S40, C41, R42, C46, T48, C49, D62, D67, D69, Q70

Non-conservative mutations at these positions resulted in proteins that were 20–67% as effective as Fd in their ET interactions with either recFNR or natFNR (Table 5). Although no single mutations were made at position 32, the E31K/E32K double mutant was shown to have only

54% of the ET reactivity observed for Fd (Table 5). Since E31K was shown to be unimportant in the interaction (Section 4.3; Table 5), it was concluded that E32 may play a role in the ET interaction of Fd with FNR, assuming that the reduction potential or binding affinity have not been deleteriously altered by the mutation. Inasmuch as E32 is not at the complex interface in the crystal structure [27], it is possible that this double charge-reversal mutation alters the molecular dipole of the Fd such that the mutual orientation of the two proteins is adversely affected.

In *Anabaena* Fd, the local secondary structure of the [2Fe–2S] cluster binding loop forces F39 into a solvent-exposed position. It had been noted that "one potential role of such a conserved, solvent-exposed aromatic amino acid may be in redox partner recognition" [51]. The reduced reactivity of F39A (Table 5) is consistent with this possibility. The reason for the altered reactivity of the S40A mutant is not clear at present.

Anabaena Fd contains only four Cys residues and these are all involved in ligating the [2Fe–2S] cluster. In order to investigate the possible importance of the Cys sulfur atom, each of these positions has been individually mutated to a Ser. ^{1}H NMR spectroscopy has been carried out on these mutants [87] and it was demonstrated that in vitro self-assembly of the iron–sulfur cluster occurs upon addition of iron and inorganic sulfur to the apoprotein of these mutants. Thus, Ser can substitute for Cys as one of the ligands to the iron–sulfur cluster. However, cluster stability is clearly diminished by such substitution.

Instability of the C79S mutant precluded studies of its ET reactivity. Instability of the C41S and C79S mutants also prevented measurement of their reduction potentials. Although the K_d values were not determined for the oxidized proteins, the ET reactivity of the three mutants for which transient kinetic data were obtainable [75] did not correlate with the K_d value determined for the transient ET complex (Fd_{red}:FNR_{ox}).

The immediate environment of the [2Fe–2S] cluster is a major determinant of the absorption spectral properties of the protein. Thus, it is not unexpected that the UV–vis [87] and CD spectra [75] of the Cys mutants are different from each other and from Fd. These spectral differences are a consequence of perturbations of the electronic character of the [2Fe–2S] cluster and are not reflected in the X-ray crystal structures. They are most likely due to altered symmetry of the [2Fe–2S] cluster and to different energies of the ligand → Fe charge-transfer transitions, caused by substitution of oxygen for sulfur as one of the ligands to the cluster. Such electronic alterations may play a part in the moderately reduced ET reactivity of these mutants with FNR, as well as in the altered reduction potential measured for the C49S mutant.

R42 forms a hydrogen bond through its amide nitrogen to one of the inorganic sulfurs of the [2Fe–2S] cluster [88]. R42 is also involved in a salt bridge with E31 and this electrostatic interaction is part of the aforementioned [2Fe–2S] cluster binding loop thought to stabilize the Fd molecule [51]. It has been suggested that R42 might play an important role in certain physiological functions and in the proper folding of the Fd molecule [89]. The R42A, R42H and R42E mutants were constructed. Of these, R42E was about half as effective as Fd in ET, whereas R42A and R42H were both somewhat more reactive in ET to natFNR relative to Fd (Table 5). The R42A result implies that neither the presence of a positive charge at this position nor the R42–E31 salt linkage is required for rapid ET with natFNR. This is in agreement with the *Anabaena* Fd/FNR crystallographic model [27] in which the Fd R42 side chain is not involved in the interaction. Therefore, the lowered reactivity observed for the R42E mutant may be due to a long-range repulsive electrostatic interaction between the proteins in the intermediate complex that alters their mutual orientation.

The crystallographic structure of the FNR/Fd complex from maize [21] reveals that Arg 40 (equivalent to Arg42 in *Anabaena*) and Glu 29 (homologous to Glu31 in *Anabaena*) of the Fd molecule form an intermolecular salt bridge with Lys 304 of FNR (Lys293 in *Anabaena*). It was proposed that this structural feature may be related to the redox potential shift observed in the free Fd_{sp} relative to that found in the FNR-bound state.

T48 is part of the cluster binding loop of Fd. Altered complex stability or an altered protein–protein orientation in the transient ET complex could be responsible for the lowered reactivity of the T48A mutant.

Although the binding of $D62K_{ox}$ to $natFNR_{ox}$ was not measured, the value of K_d determined for the intermediate ET complex ($D62K_{red}$:$natFNR_{ox}$) was somewhat smaller than that for Fd with natFNR [74]. Thus, it is probable that binding is also not the cause of the reduced reactivity of D62K. Again it appears that alterations in protein–protein orientation are mainly involved. D62 is part of the complex interface [27] and it is likely that the reduced ET reactivity is attributable to the charge reversal at this position. However, stereochemical factors may also be playing a role in the observed kinetic effect.

The D67K and D69K mutants were both significantly hindered in their ET interactions with natFNR (Table 5), in contrast to D68K (see Section 4.3; Table 5). The effects for D67K and D69K were approximately additive in the D67K/D69K double mutant. Interestingly, at low μ values, the impairment due to the D69K mutation was partially overcome by the highly reactive D68K mutation (Section 4.3) in the D68K/D69K double mutant [90]. However, including the D68K mutation in a triple mutant, D67K/D68K/D69K, did not overcome the impairment caused by the D67K and D69K mutations. The binding constants were measured for each of these oxidized mutant proteins (except D67K/D68K/D69K, for which no binding was observed) with $natFNR_{ox}$, and in each case the binding was at least as tight as it was for natFd [90].

D67 and D69 (as well as D68) are at the edge of the interface in the crystalline complex [27] (see Fig. 1B). It is

not surprising, therefore, that D67K and D69K have an effect on ET with natFNR, decreasing reactivity by 60% and 40%, respectively. Due to the electrostatic forces known to be involved in the Fd/FNR interaction, it is likely that these effects are related to the reversal in charge at these sites. However, it must be kept in mind that stereochemical factors may also come into play in cases where side chains that are sterically quite different, such as Asp and Lys, are exchanged. Further mutational studies would be required to sort this out.

The K_d value obtained at $\mu = 100$ mM for the intermediate $Q70K_{red}$:$natFNR_{ox}$ complex was found to be less than 50% smaller than the value found for Fd [74]. Thus, Q70 only moderately influences the Fd/FNR interaction.

4.3. Unimportant Fd residues—D28, E31, D36, A43, A45, D68, T78, H92, E95, Y98

Mutations made at these positions were 68–120% as effective as Fd in their ET interactions with either recFNR or natFNR (Table 5). It is noteworthy that A43 and A45 are part of the cluster binding loop of Fd. Although D68 is at the edge of the interface in the crystalline complex [27], electron density for the D68 side chain is not visible in the crystalline complex. As shown above (Section 4.2), charge-reversal mutations of the D67 and D69 residues moderately impair the ET interaction. However, the D68K mutant was more effective in ET than Fd (Table 5). Thus, the effects of the same mutation at contiguous sites are opposite. These results are similar to those obtained for the wt-like E95K mutant (see Table 5) compared to the highly impaired E94K mutant (Section 4.1, Table 5), and again point to a high degree of structural specificity within the protein–protein interaction surface during ET, as well as to a correspondingly large influence of the mutual orientation of the two proteins on the reaction rate. The K_d values calculated from the kinetics for the intermediate ET complexes involving each of these mutants were found to be very similar to that of Fd [74].

Y98 is the terminal amino acid in *Anabaena* Fd and occupies a position at the periphery of the complex interface [27]. Results for the Y98A mutant lead to the conclusion that the identity of the terminal amino acid in Fd is relatively unimportant for its ET interaction with recFNR.

5. Kinetic assessment of the importance of various amino acid residues in FNR

5.1. Critical FNR residues—R16, K72, K75, L76, L78, E301

Non-conservative mutations of these residues resulted in proteins that were 0.7–13% as effective as recFNR in their ET interactions with Fd_{red} (Table 6), illustrating the critical nature of the amino acid side chains at these positions. R16E and K72E were also shown to be significantly impaired in steady-state $NADP^+$ photoreduction assays [72]. The ET reactivity of these mutants with Fd_{red} as determined by laser flash photolysis (Table 6) correlated well with K_d values measured for complex formation between the oxidized proteins at $\mu = 12$ mM [91].

The K75E mutant was also shown by both steady-state [40,72] and transient kinetic measurements [65,91,92] to be highly impaired in its ET interaction with Fd. Laser flash photolysis showed the reactivity to be about 1% of that observed for recFNR (Table 6). To illustrate this, a transient decay curve for this reaction is shown in Fig. 5.

As noted above, the μ dependence of k_{obs} for the reaction of recFNR with Fd is clearly biphasic (Fig. 3), due to stabilization of non-optimal complexes by strong electrostatic interactions at low μ values. The R16E, K72E and K75E mutations altered the electrostatic contributions stabilizing the ET complexes such that the biphasic μ dependencies were eliminated. For R16E and K75E, the ET complexes that were formed at low μ (12 mM) were more reactive than for recFNR, but reactivity dropped off rapidly at increasing μ values. Electrostatic surface potential calculations [91] showed that R16, K72 and K75 lie in a region of the protein surface where positive charge predominates, and charge reversal would therefore have a large effect on the local surface electrostatic potential. Clearly, ET reactivity was strongly affected by these charge reversals. This is in accordance with the major role of the N-terminal domain (residues 1–138) of FNR in the interaction with Fd within the crystalline complex [27]. It should be kept in mind that steric effects may also interfere with the formation of productive ET complexes.

The conservative mutant K75R reacted much like recFNR, whereas K75Q and K75S were only moderately hindered (Table 6). Steady-state kinetic studies, utilizing the diaphorase activity with DCPIP as an electron acceptor, also

Table 6
Relative reactivities of FNR mutants in their ET reactions with Fd as studied by laser flash photolysis[a]

FNR	k_{rel}	FNR	k_{rel}	FNR	k_{rel}
R16E[b]	0.10	L76V[c]	0.56	K138E[b]	0.31
K72E[b]	0.13	L78A[c]	0.69	E139D[d]	0.76
K75E[e]	0.007	L78D[c]	0.13	E139K[d]	0.18
K75R[e]	0.76	L78F[c]	0.31	E139Q[d]	0.60
K75Q[e]	0.24	L78S[c]	0.89	R264E[b]	0.27
K75S[e]	0.24	L78V[c]	0.73	K290E[b]	0.20
L76A[c]	0.87	R100A[f]	1.00	K294E[b]	0.40
L76D[c]	0.04	V136A[c]	0.87	E301A[g]	0.01
L76F[c]	0.78	V136L[c]	0.89		
L76S[c]	0.89	V136S[c]	0.71		

[a] Relative reactivities were calculated according to footnote a in Table 5.
[b] From Ref. [91].
[c] From Ref. [64].
[d] From Ref. [95].
[e] From Ref. [65].
[f] From Ref. [66].
[g] From Ref. [63].

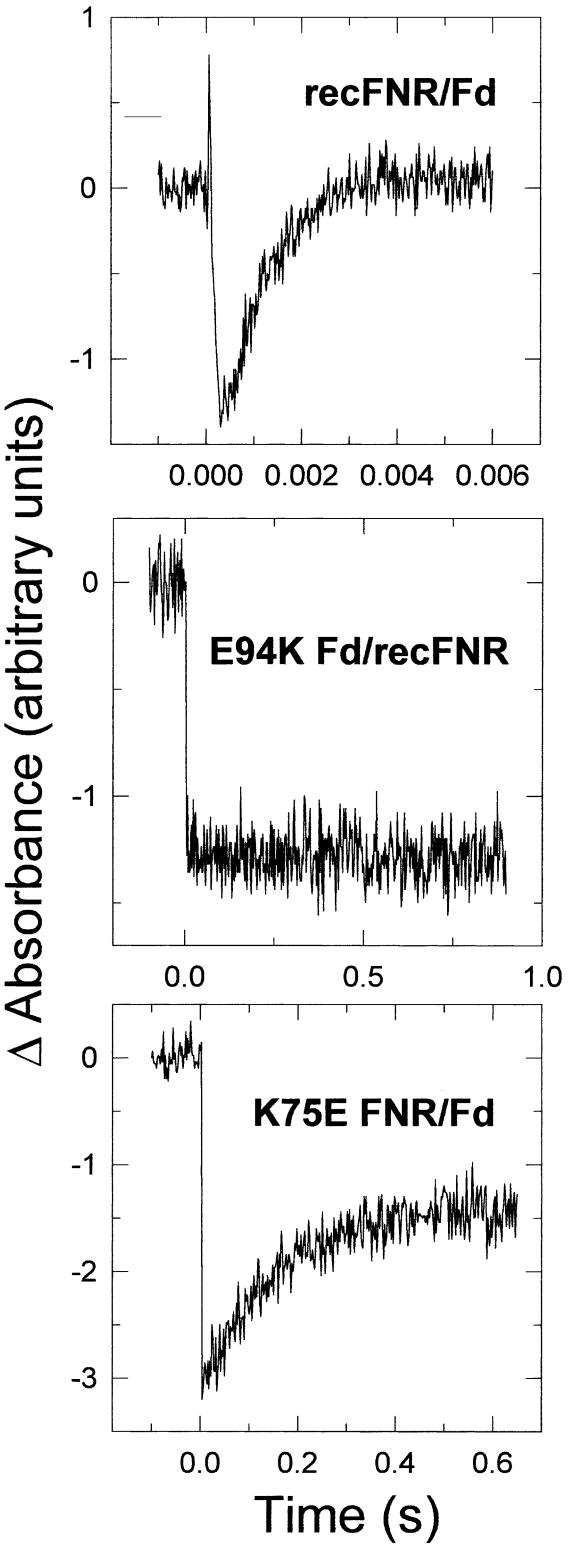

Fig. 5. Transient decay curves for 5 μM recFNR + 40 μM Fd (top), 20 μM recFNR + 40 μM E94K Fd (middle) and 5 μM K75E FNR + 40 μM Fd (bottom). The value of μ was 100 mM. Other solution conditions were as in Fig. 3. The monitoring wavelength was 507 nm, showing the reduction of Fd_{ox} by dRfH•, followed by (top and bottom panels) the oxidation of Fd_{red} by FNR_{ox}.

showed that removal of the positive charge at position 75 of FNR impaired the reaction, and that the reaction was not measurable for the K75E mutant [65].

Relative K_d values for complexation of the oxidized K75 mutant proteins with Fd_{ox} (including the highly impaired K75E, for which complex formation was not measurable), correlated well with their relative ET reactivities [65]. In the crystalline complex [27], K75 forms a salt bridge with Fd E94 at the periphery of the interface and this charge-pair plays a structural role in the association. As noted above (Section 4.1), charge-reversal mutation of Fd E94 has shown this interaction to be crucial for Fd/FNR ET (Table 5). Taken together, these results clearly indicate that the charge complementarity of FNR K75 and Fd E94 is critical for binding Fd and FNR during ET. It is noteworthy, however, that ET reactivity was not restored when K75E FNR was reacted with E94K Fd (unpublished observations). This may be because charges surrounding the mutation sites in the two proteins were disruptive to the attractive electrostatic interaction that could occur between the mutated residues, i.e. simply reversing the charges at these two individual sites on the proteins could not restore the attractive electrostatic interaction.

Of the mutations made at L76, the strongly diminished reactivity of L76D in ET from Fd_{red} measured by laser flash photolysis is most striking (Table 6). A high degree of impairment of the reactions between L76D and Fd was also observed in stopped-flow kinetic experiments, as well as in the diaphorase and NADPH-dependent cytochrome *c* reductase steady-state assays [64]. The K_d values measured for complexation of the oxidized Ser, Ala, Val and Phe mutants at position 76 with oxidized Fd varied by less than a factor of three from the value obtained for recFNR [64]. In contrast, the binding of L76D to Fd could not be detected. It is significant that the introduction of a negative charge at position 76 results in such a highly impaired mutant. This is consistent with the disruption of hydrophobic interactions by this mutation (see below).

Similarly, an Asp substitution at position L78 was shown by laser flash photolysis to cause a high degree of impairment in the ET interaction with Fd_{red} (Table 6). Other more conservative mutations at this site caused only small to moderate reductions in ET reactivity. Stopped-flow kinetic experiments, as well as the steady-state diaphorase and NADPH-dependent cytochrome *c* reductase activities also showed L78D to be highly impaired, as was observed for the L76D mutant. This mutation introduces a negatively charged side chain in an area near the FAD cofactor that is involved in hydrophobic contacts at the Fd/FNR interface in the crystalline complex [27] (see below). Again, this would be expected to be disruptive. No binding to Fd could be detected by difference absorbance measurements for L78D, again suggesting the importance of hydrophobic forces in the protein–protein interaction. The significantly decreased ET reactivities observed by laser flash photolysis for the mutants in which a negative charge was substituted for L76

and L78 are consistent with steady-state and stopped-flow kinetic results obtained with these mutants [64].

Double mutations at positions L76 and L78 were produced by the simultaneous introduction of two Asp or two Phe residues. The introduction of two negatively charged residues completely inhibited complex formation and ET with Fd. This is consistent with a major alteration found in the calculated electrostatic surface potential of the enzyme near the flavin ring using the three-dimensional structure of the mutant [64]. The L76F/L78F mutant, however, was still able to interact with Fd, although its complex with Fd is less effective for ET, presumably due to a different mutual orientation of the cofactors caused by steric interferences [64].

The E301A mutant was about 1% as active as recFNR in its ET interaction with Fd (Table 6). The steady-state photoreduction of $NADP^+$ was not hindered to this same extent, however, presumably because the rate-determining step in the more complex steady-state system is something other than ET from Fd_{red} to $FNR_{ox.}$ The K_d value for complex formation with Fd measured for E301A was larger than that measured for natFNR by a factor of two [63], but this cannot account for the very large decrease in ET reactivity measured by laser flash photolysis.

Steady-state experiments indicated that the semiquinone state of the FAD was significantly destabilized in the E301A mutant relative to recFNR. This had also been seen in three of the four mutants made at E312 in the spinach protein [93], but not to the same extent as observed for the *Anabaena* protein, which showed no semiquinone accumulation at all during photoreduction [63]. It would thus appear that lack of stabilization of the semiquinone state of E301A is the principal reason for the highly hindered ET reactivity of this FNR mutant.

The X-ray crystal structure of FNR_{sp} [24] suggested that E312 might be involved in proton transfer to N-5 of the isoalloxazine ring of FAD via S96. In *Anabaena* FNR, E301 appeared to be a good candidate to transfer protons to the isoalloxazine N-5 of FAD via S80 [18]. However, subsequent kinetic characterization and X-ray crystal structure determinations of four spinach E312 mutant proteins [93,94] led to the conclusion that this residue does not act as a proton donor during catalysis in this species, but is involved in binding NADP(H). It was also concluded that the charge of E312 contributes to establishing the redox potential of the flavin semiquinone, and that the side chain of E312 has little effect on the affinity of FNR for Fd, but does influence ET between the two proteins. In *Anabaena* FNR, although it is clear that E301 is a critical residue in the Fd/FNR interaction, it could not be determined [63] whether or not this residue is involved in transferring protons from the external medium via S80 to the N-5 position of the isoalloxazine ring of the FAD during semiquinone formation. In the Fd/FNR crystalline complex [27], the carboxylic group of Glu301 is no longer exposed to solvent but is hydrogen-bonded to the hydroxyl oxygen of Fd Ser64, which in turn is exposed to solvent. This suggests a possible proton transfer pathway between the external medium and the FNR isoalloxazine N-5 via Ser64 of Fd and the Glu301 and Ser80 side chains of FNR. It is noteworthy that the crystal structure of a pea FNR mutant (Y308S) in complex with $NADP^+$ showed the residue equivalent to E301 (i.e. E306) to be hydrogen-bonded to the FAD carboxamide group [22]. The conclusion was that this residue is primarily involved in nicotinamide binding.

In the crystal structure of the *Anabaena* E301A mutant, although no significant folding differences were observed compared to recFNR [76], conformational differences were found for the side chain of a nearby residue, E139. In the mutant, this points toward the FAD, is stabilized by a network of five hydrogen bonds to several H_2O molecules, and is connected to the S80 side chain through a series of three H_2O molecules. It was hypothesized that in the mutant, the E139 side chain may carry out some of the functions performed by the E301 side chain in the recFNR. As will be shown below, mutation of E139 in recFNR has unusual effects on ET kinetics.

5.2. Moderately important FNR residues—K138, E139, R264, K290, K294

Non-conservative mutations at these residues caused the ET reactivity with Fd_{red} to be reduced to 18–40% of that observed with recFNR (Table 6), as measured by laser flash photolysis. K138E was also evaluated by steady-state and stopped-flow techniques [72,92], which revealed moderate impairment of several reactions involving Fd. The reduced ET reactivity of K138E correlated with increased K_d values for Fd complex formation with the oxidized protein at $\mu = 12$ mM. Although K_d was not determined at high μ values, it was presumed that weakened binding was responsible for the lack of saturation behavior for K138E observed in the k_{obs} vs. FNR concentration dependence under these conditions [91].

Transient kinetic measurements showed E139K to be significantly impaired in its ET interaction with Fd_{red} (Table 6). In the crystalline complex [27], this residue is located at the periphery of the interaction site. However, no direct contact occurs with Fd although the distance from FNR E139 Oε to the Fd S61 main chain carbonyl oxygen is only 4.6 Å. This allows it to be mutated to a Lys or a Gln without sterically impairing the Fd/FNR association.

In the E139K and E139Q mutations, the change in charge adversely affects the electrostatic interactions of the proteins. At low μ (12 mM) the ET interaction with Fd was highly impaired, and the dependency of k_{obs} on FNR concentration showed strong upward curvature at protein concentrations >10 μM [95]. At values of μ> 200 mM ET reaction rates approach those observed with recFNR and normal saturation kinetics were obtained. The E139Q mutant was also significantly hindered at low values of μ and low protein concentrations [95] and showed a smaller

degree of upward curvature in its dependency of k_{obs} on FNR concentration. Like E139K, the E139Q mutant had normal saturation kinetics at higher values of μ. The μ dependency of k_{obs} was quite broad for this mutant and it was thought that loss of electrostatic repulsion between E139 and the Fd surface was the cause of this. It is expected that both attractive and repulsive forces are active in orienting the proteins, giving rise to a broadened μ dependency in this mutant. This has also been suggested for the interaction of the [3Fe–4S] FdI from *Azotobacter vinelandii* with NADPH-ferredoxin reductase [96]. The E139D mutant, as well as recFNR (which was reevaluated after the E139K results were obtained), showed a smaller degree of upward curvature at FNR concentrations >30 μM at $\mu = 12$ mM, and also showed saturation kinetics at higher values of μ.

The kinetic behavior of the E139 mutants was explained as follows [95]. At low μ, the proteins form a complex in which the mutual orientation of the redox cofactors of the proteins is so far from optimal that they are almost unreactive in ET (e.g. k_{obs} for E139K was less than 20 s^{-1} at the highest FNR concentration used, compared to approximately 1100 s^{-1} for recFNR). At increasing FNR concentrations, added FNR_{ox} is able to oxidize the bound Fd_{red} in the slowly reacting complex because the iron–sulfur center is oriented away from the FNR surface, thereby leading to increased rates for the production of FNR_{red}. This ternary reaction is the source of the upward curvature in the FNR concentration dependence. The degree of reactivity observed at low values of μ depended on the particular amino acid substitution, with E139K being by far the most unreactive. Only a small amount of non-linearity at the highest FNR concentrations was observed for recFNR. As the value of μ was increased, electrostatic forces involved in stabilizing the complex were weakened and the proteins could rearrange to a more reactive ET complex in which the iron–sulfur center is pointed towards the FNR surface. Thus, electrostatic forces were responsible for controlling the specific geometry at the interface between the proteins, which in turn determined the rates of ET occurring within the complex. Ternary reactions involving ET proteins are not unique to this protein pair and have been previously described for the cytochrome *c*:cytochrome *c* peroxidase system [97–101]. There was no evidence for a stable ternary complex formed between Fd and two molecules of E139K and thus the reaction proceeded via a collisional interaction. These results demonstrate the importance of E139 for competent complex formation between Fd and FNR, as well as the strong influence of electrostatic interactions on the ET behavior of this protein pair.

R264 has previously been suggested to play a role in Fd recognition [18]. In agreement with this the R264E mutant was shown by laser flash photolysis (Table 6), stopped-flow and steady-state kinetic measurements [66] to be appreciably decreased in its ET reactivity with Fd_{red}. The K_d value for the binding of $R264E_{ox}$ to Fd_{ox} was essentially the same as that found for recFNR, and the K_d value determined for the transient ET complex was only a factor of two larger in the case of the mutant. However, the dependence of k_{obs} on μ indicated that electrostatic interactions in the complex have been weakened and that structural rearrangement leading to more productive ET complexes occurred at lower salt concentrations relative to recFNR. Electrostatic surface potential calculations on R264E revealed a significant change in polarity in the FAD environment, which was suggested to have a destabilizing effect on the complex [66]. These latter two observations led to the conclusion that the altered charge properties of this mutant are responsible for the decreased effectiveness of the ET interaction with Fd. R264 (like F65 in Fd) is one of the most important interface residues in the Fd/FNR crystalline complex [27], having 12 van der Waals (VDW) contacts and two direct hydrogen bonds. However, since this residue is located at the periphery of the interaction site, a mutation to Glu could be made without stereochemically impairing the formation of the Fd/FNR complex, although such a mutation would greatly decrease the number of VDW contacts and eliminate the hydrogen bonds. This apparently results in a less-than-optimal mutual orientation of the proteins in the complex.

The ET interactions of K290E and K294E with Fd_{ox} were evaluated by steady-state, laser flash photolysis and stopped-flow techniques [72,91,92]. Laser flash photolysis showed these mutants to be moderately impaired (Table 6). The ET reactivity correlated well with K_d values measured for the oxidized proteins at $\mu = 12$ mM. K_d values were not determined for these mutants at high μ values, but it was presumed that weakened binding was responsible for the lack of saturation behavior for K294E observed in a plot of k_{obs} vs. FNR concentration.

Charge reversal mutations at K138, R264, K290 and K294 altered the electrostatic forces stabilizing the ET complexes such that the biphasic μ dependency observed for recFNR (Fig. 3) was either eliminated or, in the case of R264E, minimized [91]. As a consequence, the ET complexes that were formed for these mutants at low μ were more reactive than for recFNR. Electrostatic surface potential calculations showed that these four residues lie in regions of the protein surface that have a large negative potential [91]. Thus, introduction of additional negative charge in these areas would have relatively small effects, although it should also be kept in mind that stereochemical effects may interfere with the formation of productive ET complexes.

5.3. Unimportant FNR residues—R100A, V136

Non-conservative mutants at these positions were 71–100% as effective as wt FNR in accepting an electron from Fd_{red} (Table 6). R100 in *Anabaena* FNR and the equivalent residue in FNR_{sp} (K116) have been shown by chemical modification studies to be involved in the interaction of

FNR with the $NADP^+$ cofactor [102–104], and the role of the side chain of this residue in binding the pyrophosphate group of NADP(H) has also been probed by site-directed mutagenesis [66,105].

V136 is part of the hydrophobic core formed at the interface upon crystalline complex formation [27]. However, Leu, Ala and Ser mutations at this position were shown by laser flash photolysis to have only small effects on ET with Fd_{red} (Table 6). Consistent with this, the K_d values for the complexes formed between the oxidized forms of these mutants and oxidized Fd were very similar to the value obtained for recFNR [64]. It should be noted that no mutations have been made which placed a charge at this position.

6. Correlations with structural information

Only a limited number of the mutations in both Fd and FNR resulted in large kinetic effects on the ET reaction between the two proteins. In Fd (see Fig. 1A), several of the critical residues lie close to the partially exposed [2Fe–2S] cluster, with the region immediately below the cluster being the most important (S47, F65, E94). In FNR (Fig. 1C), the most important residues lie within and at the right-hand periphery of the concave cavity of the FNR surface that contains the exposed edge of the flavin isoalloxazine ring (R16, K72, K75, L76, L78, E301). It is important to note that all of these residues are found at the FNR–Fd interface in the crystalline complex [27].

In the complex crystal structure, depicted in Fig. 2A and B, Fd is seen to bind to the concave surface of the FNR molecule from which the exposed dimethylbenzene portion of the isoalloxazine ring projects. The closest distance from the [2Fe–2S] cluster to the flavin is 7.4 Å (from the S2 atom of the cluster to the C8-methyl of the FAD). This is consistent with evidence that indicates that the C8-methyl group of the isoalloxazine ring is involved in flavoprotein ET [106]. The redox centers are separated by a main chain segment of the Fd molecule consisting of A43–G44–A45, and thus there is little steric hindrance to electron flow between the cofactors. This suggests a relatively rapid direct electron transfer between them, which is consistent with the observed maximal k_{et} of 5500 s^{-1} [33]. It is also significant that Fd undergoes a redox-linked conformational change upon ET [12,27]. This change is centered at the core of the Fd/FNR interfacial region in the *Anabaena* complex and thus may be involved in the separation of the two proteins subsequent to ET.

The protein–protein interface in the crystalline complex contains both a core of hydrophobic side chains (including F65 of Fd and L76, L78 and V136 of FNR), as well as acidic residues of Fd (D62, D67, E94) and acidic (E267, E301) and basic (R16, K75, R264, K293) residues of FNR. These groups interact with each other either directly or through bridging water molecules. Thus, D67 of Fd interacts with R16 of FNR; D62 of Fd hydrogen bonds with R264 of FNR; and E94 of Fd forms a salt linkage with K75 of FNR. The interface between the *Anabaena* proteins is also stabilized by hydrophobic interactions involving long side chains such as R264 of FNR (which makes 11 VDW contacts with Fd), and the loss of about 10 water molecules upon complex formation [27]. This latter point is in agreement with calorimetric experiments on the complex of the spinach proteins [32]. Some of these interactions are shown in Fig. 2B.

As noted above, mutation of F65 of Fd to either Ala or Ile decreases ET reactivity with FNR by four orders of magnitude (Table 5). This is consistent with a decrease in the hydrophobic interaction at the FNR–Fd complex interface. Of the 11 VDW contacts with FNR made by F65, seven are with L78 and two are with V136. The observed losses of ET reactivity for mutants in which an Asp substitution is made at L78 and a Ser substitution at V136 are also consistent with a disruption of these hydrophobic interactions. In this context, it is important to note that an Asp substitution at L76 also severely impairs ET to Fd. Although L76 does not directly contact F65 (the closest distance between F65 and L76 is 4.8 Å), it does lie in the complex interface (Figs. 2B and 4). It is also close to the C-terminus of Fd. The latter point suggests that placing a negative charge in this position might lead to serious disruption of the complex via electrostatic repulsion with the negatively charged C-terminal carboxylate. As noted above, the identity of the side chain of the C-terminal residue in Fd is not critical.

Fig. 1B and D show space-filling models of Fd and FNR, respectively, with the side chains of residues located within the protein/protein interface in the crystalline complex colored red. Comparison of these models with Fig. 1A and C demonstrates a strong correlation between deleterious effects on ET reactivity and location of the residues at the complex interface. We conclude from these correlations that the crystalline Fd/FNR complex is a viable model for a productive intermediate formed during ET. In this context, it should be noted that the critical S47 residue of Fd, as well as the moderately important C46, are not colored red in Fig. 2A. This is because, although they are positioned in front of FNR in the complex, there is a "cavity" separating these residues from direct contact with the FNR surface. Another apparent discrepancy involves the K72 residue in FNR, which was shown to be crucial for ET but is not located at the complex interface. The impaired reactivity of the K72E mutant can be attributed to a disruptive long-range electrostatic interaction with the negatively charged Fd surface. Similar long-range electrostatic effects may explain why some additional residues located close to but not within the complex interface in FNR (such as K290 and K294) and in Fd (Q70, which was mutated to a Lys) showed moderate impairment in ET reactivity upon non-conservative mutation. Other residues in this category are F39, S40 and T48 of Fd, all of which show moderate impairment in ET reactivity

upon non-conservative mutation but are not directly located at the complex interface. However, these latter three residues are part of the [2Fe–2S] cluster binding loop, and are located 4.5–5.0 Å from the cluster. Thus, a direct effect on the properties of the cluster may be involved in their influence on reactivity.

The X-ray structure of a second Fd/FNR complex, involving proteins from maize leaves, has recently been determined [21]. As in the *Anabaena* protein complex, the interface consists of both electrostatic and hydrophobic interactions near the prosthetic groups, the latter involving mainly the non-polar FNR patch, Val 92, Leu 94 and Val 151. The prosthetic groups are again close to each other so that fast ET is possible. However, superposition of the FNR molecules of each of the two complexes reveals that the Fd molecules are rotated by an angle of 96°. This indicates that many of the specific interactions within the complexes are not the same. In particular, Y63, corresponding to the critical F65 residue of *Anabaena* Fd, is no longer located between the prosthetic groups of the two proteins and is involved to a lesser extent in hydrophobic interactions with FNR. Moreover, E92, the maize equivalent of the critical E94 residue of *Anabaena* Fd, is not involved at all in the FNR interaction. In this regard, kinetic studies have shown significant differences between the *Anabaena* and spinach protein systems in the relative contributions of electrostatic and hydrophobic interactions during ET [31], indicating species-specific differences in the protein–protein interactions.

These results show that the major features shared by the *Anabaena* and maize Fd/FNR crystalline complexes are a hydrophobic patch centered on FNR and the close proximity of the two redox centers, which allows fast electron exchange. Thus, despite their structural differences, the *Anabaena* and maize leaf complexes may both represent functional ET intermediates. This viewpoint is further supported by the fact that the mutual orientation within a crystalline complex of the proteins obtained from maize roots differs from that found in the maize leaf proteins (T. Hase, personal communication). Thus, the crucial parameters that have been conserved during evolution may simply be close prosthetic group proximity and a non-polar environment during the ET process.

Acknowledgements

The authors thank Dr. Michel Frey for his critical reading of the manuscript and for many helpful discussions.

This research was supported by grants from the National Institutes of Health (DK15057 to G.T.), from the Comisión Interministerial de Ciencia y Tecnología (BIO2000-1259 to C.G.-M.), from the Diputación General de Aragón (P006/2000 to M.M.) and by the CEA, the CNRS and the Ministère de l'Education Nationale de la Recherche et de la Technologie (to R.M.).

References

[1] H. Matsubara, K. Saeki, in: R. Cammack, A.G. Sykes (Eds.), Advances in Inorganic Chemistry, Iron–Sulfur Proteins, vol. 38, Academic Press, San Diego, CA, USA, 1992, pp. 223–280.
[2] M. Martínez-Júlvez, J.K. Hurley, G. Tollin, C. Gómez-Moreno, M.F. Fillat, Biochim. Biophys. Acta 1297 (1996) 200–206.
[3] M.F. Fillat, E. Flores, C. Gómez-Moreno, Plant Mol. Biol. 22 (1993) 725–729.
[4] T. Tsukihara, K. Fukuyama, M. Mizushima, T. Harioka, M. Kusunoki, Y. Katsube, T. Hase, H. Matsubara, J. Mol. Biol. 216 (1990) 399–410.
[5] W.R. Rypniewski, D.R. Breiter, M.M. Benning, G. Wesenberg, B.-H. Oh, J.L. Markley, I. Rayment, H.M. Holden, Biochemistry 30 (1991) 4126–4131.
[6] B.L. Jacobson, Y.K. Chae, J.L. Markley, I. Rayment, H.M. Holden, Biochemistry 32 (1993) 6788–6793.
[7] S. Ikemizu, M. Bando, T. Sato, Y. Morimoto, T. Tsukihara, K. Fukuyama, Acta Crystallogr. D50 (1994) 167–174.
[8] K. Fukuyama, N. Ueki, H. Nakamura, T. Tsukihara, H. Matsubara, J. Biochem. 117 (1995) 1017–1023.
[9] F. Frolow, M. Harel, J.L. Sussman, M. Mevarech, M. Shoham, Nat. Struct. Biol. 3 (1996) 452–458.
[10] C. Binda, A. Coda, A. Aliverti, G. Zanetti, A. Mattevi, Acta Crystallogr. D54 (1998) 1353–1358.
[11] M.T. Bes, E. Parisini, L.A. Inda, L.M. Saraiva, M.L. Peleato, G.M. Sheldrick, Struct. Fold Des. 7 (1999) 1201–1211.
[12] R. Morales, M.-H. Charon, G. Hudry-Clergeon, Y. Pétillot, S. Norager, M. Medina, M. Frey, Biochemistry 38 (1999) 15733–15764.
[13] C. Lelong, P. Sétif, H. Bottin, F. André, J.-M. Neumann, Biochemistry 34 (1995) 14462–14473.
[14] B. Baumann, H. Stricht, M. Schärpf, M. Sutter, W. Haehnel, P. Rösch, Biochemistry 35 (1996) 12831–12841.
[15] H. Hatanaka, R. Tanimura, S. Katoh, F. Inagaki, J. Mol. Biol. 268 (1997) 922–933.
[16] C. Im, G. Liu, C. Luchinat, A.G. Sykes, I. Bertini, Eur. J. Biochem. 258 (1998) 465–477.
[17] B. Schrautemeier, H. Böhme, FEBS Lett. 2560 (1985) 304–308.
[18] L. Serre, M.D. Vellieux, M. Medina, C. Gómez-Moreno, J.C. Fontecilla-Camps, M. Frey, J. Mol. Biol. 263 (1996) 20–39.
[19] G. Sridhar Prasad, N. Kresge, A.B. Muhlberg, A. Shaw, Y.S. Jung, B.K. Burgess, C.D. Stout, Protein Sci. 7 (1998) 2541–2549.
[20] M. Ingelman, V. Bianchi, H. Eklund, J. Mol. Biol. 268 (1997) 147–157.
[21] G. Kurisu, M. Kusunoki, E. Katoh, T. Yamazaki, K. Teshima, Y. Onda, Y. Kimata-Ariga, T. Hase, Nat. Struct. Biol. 8 (2001) 117–121.
[22] Z. Deng, A. Aliverti, G. Zanetti, A.K. Arakaki, J. Ottado, E.G. Orellano, N.B. Calcaterra, E.A. Ceccarelli, N. Carrillo, P.A. Karplus, Nat. Struct. Biol. 6 (1999) 847–853.
[23] A. Dorowski, A. Hofmann, C. Steegborn, M. Boicu, R. Huber, J. Biol. Chem. 276 (2001) 9253–9263.
[24] C.M. Bruns, P.A. Karplus, J. Mol. Biol. 247 (1995) 125–145.
[25] A. Karplus, M.J. Daniels, J.R. Herriot, Science 251 (1991) 60–66.
[26] A.R. De Pascalis, I. Jelesarov, F. Ackermann, W.H. Koppenol, M. Hirasawa, D.B. Knaff, H.R. Bosshard, Protein Sci. 2 (1993) 1126–1135.
[27] R. Morales, M.-H. Charon, G. Kacholova, L. Serre, M. Medina, C. Gómez-Moreno, M. Frey, EMBO Reports 1 (2000) 271–276.
[28] G.P. Foust, S.G. Mayhew, V. Massey, J. Biol. Chem. 244 (1969) 964–970.
[29] C.J. Batie, H. Kamin, J. Biol. Chem. 259 (1984) 8832–8839.
[30] A.K. Bhattacharyya, T.E. Meyer, G. Tollin, Biochemistry 25 (1986) 4655–4661.
[31] M.C. Walker, J.J. Pueyo, J.A. Navarro, C. Gómez-Moreno, G. Tollin, Arch. Biochem. Biophys. 287 (1991) 351–358.
[32] I. Jelesarov, H.R. Bosshard, Biochemistry 33 (1994) 13321–13328.
[33] J.K. Hurley, M.F. Fillat, C. Gómez-Moreno, G. Tollin, J. Am. Chem. Soc. 118 (1996) 5526–5531.

[34] R. Morales, G. Kachalova, F. Vellieux, M.-H. Charon, M. Frey, Acta Crystallogr. D56 (2000) 1408–1412.
[35] J.K. Hurley, Z. Salamon, T.E. Meyer, J.C. Fitch, M.A. Cusanovich, J.L. Markley, H. Cheng, B. Xia, Y.K. Chae, M. Medina, C. Gómez-Moreno, G. Tollin, Biochemistry 32 (1993) 9346–9354.
[36] J. Alam, R.A. Whitaker, D.W. Krogman, S.E. Curtis, J. Bacteriol. 168 (1986) 265–1271.
[37] H. Böhme, R. Haselkorn, Plant Mol. Biol. 12 (1989) 667–672.
[38] M.F. Fillat, W.E. Borrias, P.J. Weisbeek, in: B. Curti, S. Ronchi, G. Zanetti (Eds.), Flavins and Flavoproteins 1990, Walter de Gruyter & Co., Berlin, 1991, pp. 445–448.
[39] M.F. Fillat, M.C. Pacheco, M.L. Peleato, C. Gómez-Moreno, in: K. Yagi (Ed.), Flavins and Flavoproteins 1993, Walter de Gruyter & Co., Berlin, 1994, pp. 447–450.
[40] C. Gómez-Moreno, M. Martínez-Júlvez, M.F. Fillat, J.K. Hurley, G. Tollin, in: P. Mathis (Ed.), Photosynthesis: From Light to Biosphere, vol. II, Academic Press, The Netherlands, 1995, pp. 627–632.
[41] D.B. Knaff, in: D.R. Ort, C.F. Yocum (Eds.), Oxygenic Photosynthesis: The Light Reactions, Kluwer Academic Publishers, Dordrecht, 1996, pp. 333–361.
[42] A.G. Sykes, in: H. Sigel, A. Sigel (Eds.), Metal Ions in Biological Systems, Marcel Dekker, New York, 1991, pp. 291–321.
[43] D.B. Knaff, M. Hirasawa, Biochim. Biophys. Acta 1056 (1991) 93–125.
[44] R. Cammack, in: R. Cammack, A.G. Sykes (Eds.), Advances in Inorganic Chemistry, vol. 38, Academic Press, San Diego, CA, USA, 1992, pp. 281–322.
[45] M.K. Johnson, in: R.B. King (Ed.), Encyclopedia of Inorganic Chemistry, Wiley, New York, NY, USA, 1994, pp. 1896–1915.
[46] H. Sticht, P. Rösch, Prog. Biophys. Mol. Biol. 70 (1998) 95–136.
[47] G. Zanetti, A. Aliverti, in: F. Müller (Ed.), Chemistry and Biochemistry of Flavoenzymes, vol. II, CRC Press, Boca Raton, FL, USA, 1991, pp. 305–315.
[48] N. Carrillo, R.H. Vallejos, in: J. Barber (Ed.), Topics in Photosynthesis, vol. 8, Elsevier, Amsterdam, 1987, pp. 527–560.
[49] P.A. Karplus, C.M. Bruns, J. Bioenerg. Biomembr. 26 (1994) 89–99.
[50] A.K. Arakaki, E.A. Ceccarelli, N. Carillo, FASEB J., (1997) 133–140.
[51] H.M. Holden, B.L. Jacobson, J.K. Hurley, G. Tollin, B.-H. Oh, L. Skjeldal, Y.K. Chae, H. Cheng, B. Xia, J.L. Markley, J. Bioenerg. Biomembr. 26 (1994) 67–88.
[52] C. Gómez-Moreno, M. Martínez-Júlvez, M.F. Fillat, J.K. Hurley, G. Tollin, Biochem. Soc. Trans. 24 (1996) 111–116.
[53] C. Gómez-Moreno, M. Martínez-Júlvez, M. Medina, J.K. Hurley, G. Tollin, Biochimie 80 (1998) 837–846.
[54] R.A. Marcus, N. Sutin, Biochim. Biophys. Acta 811 (1985) 265–322.
[55] G. Tollin, T.E. Meyer, M.A. Cusanovich, Biochim. Biophys. Acta 853 (1986) 29–41.
[56] C.C. Page, C.C. Moser, X. Chen, P.L. Dutton, Nature 402 (1999) 47–52.
[57] W.B. Curry, M.D. Grabe, I.V. Kurnikov, S.S. Skourtis, D.N. Beratan, J.J. Regan, A.J.A. Aquino, P. Beroza, J.N. Onuchic, J. Bioenerg. Biomembr. 27 (1995) 285–293.
[58] H.B. Gray, J.R. Winkler, Annu. Rev. Biochem. 65 (1996) 537–561.
[59] V.L. Davidson, Acc. Chem. Res. 33 (2000) 87–93.
[60] D.S. Bendall (Ed.), Protein Electron Transfer, Bioscientific Publishers, Oxford, UK, 1996.
[61] G.W. Canters, C. Dennison, Biochimie 77 (1995) 506–515.
[62] H. Matsubara, T. Hase, Protein and Nucleic Acids in Plant Systematics, in: U. Jensen, D.E. Fairbrothers (Eds.), Springer-Verlag, Berlin, 1983, pp. 168–181.
[63] M. Medina, M. Martínez-Júlvez, J.K. Hurley, G. Tollin, C. Gómez-Moreno, Biochemistry 37 (1998) 2715–2728.
[64] M. Martínez-Júlvez, I. Nogués, M. Faro, J.K. Hurley, T.B. Brodie, T. Mayoral, J. Sanz-Aparicio, J.A. Hermoso, M.T. Stankovich, M. Medina, G. Tollin, C. Gómez-Moreno, J. Biol. Chem. 276 (2001) 27498–27510.
[65] M. Martínez-Júlvez, M. Medina, J.K. Hurley, R. Hafezi, T.B. Brodie, G. Tollin, C. Gómez-Moreno, Biochemistry 37 (1998) 13604–13613.
[66] M. Martínez-Júlvez, J. Hermoso, J.K. Hurley, T. Mayoral, J. Sanz-Aparicio, G. Tollin, C. Gómez-Moreno, M. Medina, Biochemistry 37 (1998) 17680–17691.
[67] M. Medina, I.G. Bazo, M.F. Fillat, C. Gómez-Moreno, Protein Sequences Data Anal. 5 (1993) 247–252.
[68] G. Zanetti, D. Morelli, S. Ronchi, A. Negri, A. Aliverti, B. Curti, Biochemistry 27 (1988) 3753–3759.
[69] B.J. Vieira, K.K. Colvert, D.J. Davis, Biochim. Biophys. Acta 851 (1986) 109–122.
[70] I. Jelesarov, A.R. De Pascalis, W.H. Koppenol, M. Hirasawa, D.B. Knaff, H.R. Bosshard, Eur. J. Biochem. 216 (1993) 57–66.
[71] M. Medina, E. Mendez, C. Gómez-Moreno, FEBS 298 (1992) 25–28.
[72] S. Schmitz, M. Martínez-Júlvez, C. Gómez-Moreno, H. Böhme, Biochim. Biophys. Acta 1363 (1998) 85–93.
[73] A.M. Weber-Main, J.K. Hurley, H. Cheng, B. Xia, Y.K. Chae, J.L. Markley, M. Martínez-Júlvez, C. Gómez-Moreno, M.T. Stankovich, G. Tollin, Arch. Biochem. Biophys. 355 (1998) 181–188.
[74] J.K. Hurley, A.M. Weber-Main, M.T. Stankovich, M.M. Benning, J.B. Thoden, J.L. Vanhooke, H.M. Holden, Y.K. Chae, B. Xia, H. Cheng, J.L. Markley, M. Martínez-Júlvez, C. Gómez-Moreno, J.L. Schmeits, G. Tollin, Biochemistry 36 (1997) 11100–11117.
[75] J.K. Hurley, A.M. Weber-Main, A.E. Hodges, M.T. Stankovich, M.M. Benning, H.M. Holden, H. Cheng, B. Xia, J.L. Markley, C. Genzor, C. Gómez-Moreno, R. Hafezi, G. Tollin, Biochemistry 36 (1997) 15109–15117.
[76] T. Mayoral, M. Medina, J. Sanz-Aparicio, C. Gómez-Moreno, J.A. Hermoso, Proteins 38 (2000) 60–69.
[77] J.K. Hurley, M.F. Fillat, C. Gómez-Moreno, G. Tollin, Biochimie 77 (1995) 539–548.
[78] G. Tollin, J.T. Hazzard, Arch. Biochem. Biophys. 287 (1991) 1–7.
[79] G. Tollin, J.K. Hurley, J.T. Hazzard, T. Meyer, Biophys. Chem. 48 (1993) 259–279.
[80] G. Tollin, J. Bioenerg. Biomembr. 27 (1995) 303–309.
[81] R.P. Simondsen, P.C. Weber, F.R. Salemme, G. Tollin, Biochemistry 21 (1982) 6366–6375.
[82] R.P. Simondsen, G. Tollin, Biochemistry 22 (1983) 3008–3016.
[83] J.K. Hurley, H. Cheng, B. Xia, J.L. Markley, M. Medina, C. Gómez-Moreno, G. Tollin, J. Am. Chem. Soc. 115 (1993) 11698–11701.
[84] A. Aliverti, W.R. Hagen, G. Zanetti, FEBS Lett. 368 (1995) 220–224.
[85] L. Piubelli, A. Aliverti, F. Bellintani, G. Zanetti, Eur. J. Biochem. 236 (1996) 465–469.
[86] A. Aliverti, A. Livraghi, L. Piubelli, G. Zanetti, Biochim. Biophys. Acta 1342 (1997) 45–50.
[87] H. Cheng, B. Xia, G.H. Reed, J.L. Markley, Biochemistry 33 (1994) 3155–3164.
[88] L. Skjeldal, W.M. Westler, B.-H. Oh, A.M. Krezel, H.M. Holden, B.L. Jacobson, I. Rayment, J.L. Markley, Biochemistry 30 (1991) 7363–7368.
[89] T. Tsukihara, M. Kobayashi, M. Nakamura, Y. Katsube, K. Fukuyama, T. Hase, H. Matsubara, Biosystems 15 (1982) 243–257.
[90] J.K. Hurley, J.L. Schmeits, C. Genzor, C. Gómez-Moreno, G. Tollin, Arch. Biochem. Biophys. 333 (1996) 243–250.
[91] J.K. Hurley, J.T. Hazzard, M. Martínez-Júlvez, M. Medina, C. Gómez-Moreno, G. Tollin, Protein Sci. 8 (1999) 1614–1622.
[92] M. Martínez-Júlvez, M. Medina, C. Gómez-Moreno, J. Biol. Inorg. Chem. 4 (1999) 568–578.
[93] A. Aliverti, Z. Deng, D. Ravasi, L. Piubelli, P.A. Karplus, G. Zanetti, J. Biol. Chem. 273 (1998) 34008–34015.
[94] G. Zanetti, A. Aliverti, D. Ravasi, B. Curti, Z. Deng, P.A. Karplus, in: K.J. Stevenson, V. Massey, C.H. Williams (Eds.), Flavins and Flavoproteins 1996, University of Calgary Press, Calgary, Alberta, Canada, 1997, pp. 509–512.
[95] J.K. Hurley Jr., M. Faro, T.B. Brodie, J.T. Hazzard, M. Medina, C. Gómez-Moreno, G. Tollin, Biochemistry 39 (2000) 13695–13702.

[96] Y.-S. Jung, V.A. Roberts, C.D. Stout, B.K. Burgess, J. Biol. Chem. 274 (1999) 2978–2987.
[97] C.H. Kang, S. Ferguson-Miller, E. Margoliash, Biochemistry 252 (1977) 919–926.
[98] M.R. Nuevo, H.-H. Chu, L.B. Vitello, J.E. Erman, J. Am. Chem. Soc. 115 (1993) 5873–5874.
[99] M.R. Mauk, J.C. Ferrer, A.G. Mauk, Biochemistry 33 (1994) 12609–12614.
[100] J.S. Zhou, J.M. Nocek, M.L. DeVan, B.M. Hoffman, Science 269 (1995) 204–207.
[101] J.S. Zhou, S.T. Tran, G. McLendon, B.M. Hoffman, J. Am. Chem. Soc. 119 (1997) 269–277.
[102] M. Medina, E. Méndez, C. Gómez-Moreno, Arch. Biochem. Biophys. 299 (1992) 281–286.
[103] A. Aliverti, G. Gadda, S. Ronchi, G. Zanetti, Eur. J. Biochem. 198 (1991) 21–24.
[104] D. Cidaria, P.A. Biondini, G. Zanetti, S. Ronchi, Eur. J. Biochem. 146 (1985) 295–299.
[105] A. Aliverti, T. Lübberstedt, G. Zanetti, R.G. Herrmann, B. Curti, J. Biol. Chem. 266 (1991) 17760–17763.
[106] J. Fritz, F. Müller, S.G. Mayhew, Helv. Chim. Acta 56 (1973) 2250–2254.
[107] P.J. Kraulis, J. Appl. Crystallogr. 24 (1991) 946–950.
[108] E.A. Merritt, D.J. Bacon, in: C.W. Carter, R.M. Sweet (Eds.), Methods Enzymol., vol. 277, Academic Press, San Diego, 1997, pp. 505–524.
[109] M. Vidakovic Jr., G. Fraczkiewicz, B.C. Dave, R.S. Czernuszewicz, J. Germanas, Biochemistry 34 (1995) 13906–13913.
[110] J.K. Hurley, M. Medina, C. Gómez-Moreno, G. Tollin, Arch. Biochem. Biophys. 312 (1994) 480–486.